

Effect of Metallic Ions on Silk Formation in the Mulberry Silkworm, *Bombyx mori*Li Zhou,<sup>†</sup> Xin Chen,<sup>\*,†</sup> Zhengzhong Shao,<sup>†</sup> Yufang Huang,<sup>‡</sup> and David P. Knight<sup>§</sup>

The Key Laboratory of Molecular Engineering of Polymers, Department of Macromolecular Science and Department of Material Science, National Microanalysis Center, Fudan University, Shanghai, 200433, People's Republic of China, and Department of Zoology, University of Oxford, South Parks Road, Oxford OX1 3PS, U.K.

Received: February 21, 2005; In Final Form: June 21, 2005

A protein conformation transition from random coil and/or helical conformation to  $\beta$ -sheet is known to be central to the process used by silk-spinning spiders and insects to convert concentrated protein solutions to tough insoluble threads. Several factors including pH, metallic ions, shear force, and/or elongational flow can initiate this transition in both spiders and silkworms. Here, we report the use of proton induced X-ray emission (PIXE), inductively coupled plasma mass spectroscopy (ICP-MS) and atomic adsorption spectroscopy (AAS) to investigate the concentrations of six metal elements (Na, K, Mg, Ca, Cu, and Zn) at different stages in the silk secretory pathway in the *Bombyx mori* silkworm. We also report the use of Raman spectra to monitor the effects of these six metallic ions on the conformation transition of natural silk fibroin dope and concentrated regenerated silk fibroin solution at concentrations similar to the natural dope. The results showed that the metal element contents increased from the posterior part to the anterior part of silk gland with the exception of Ca which decreased significantly in the anterior part. We show that these changes in composition can be correlated with (i) the ability of  $\text{Mg}^{2+}$ ,  $\text{Cu}^{2+}$ , and  $\text{Zn}^{2+}$  to induce the conformation transition of silk fibroin to  $\beta$ -sheet, (ii) the effect of  $\text{Ca}^{2+}$  in forming a stable protein network (gel), and (iii) the ability of  $\text{Na}^+$  and  $\text{K}^+$  to break down the protein network.

## 1. Introduction

During the few past decades natural animal silks, from spiders and silkworms, have attracted considerable interest for their outstanding mechanical properties, comparable or even superior to high performance synthetic materials.<sup>1–5</sup> However, apart from the production of fine cloth for the top end of the apparel market, several factors limit the widespread adoption of silkworm silk in other commercial sectors. The main problem is that its production is labor intensive, and hence production costs are high compared to synthetic fibers. Although spider dragline silk has much better mechanical properties than silkworm silk,<sup>3</sup> its industrial exploitation faces even greater problems than that of silkworm silk. The labor costs of collecting sufficient dragline silk would be colossal.

With the development of biotechnology, partial and complete gene sequences have been reported for the major structural proteins in silks in a range of lepidopteran and spider species.<sup>6–8</sup> A number of silklike proteins with precisely specified amino acid sequences have been produced by recombinant DNA technology.<sup>9</sup> Several different methods have been tried to spin regenerated or recombinant silk proteins into silklike fibers artificially.<sup>9–13</sup> However, most of the artificial silk fibers had inferior mechanical properties compared with naturally spun silks<sup>13–16</sup> with the exception of one spun by Lazaris et al.<sup>9</sup> that showed comparable toughness and modulus to native spider dragline silks but lower tenacity. On the other hand, it has been

shown that when reeled under controlled conditions, the mechanical properties of silkworm silks approached those of spider dragline silk.<sup>3</sup> Taken together these and further observations<sup>3,17,18</sup> indicate that the mechanical properties of natural silk depend not only on the unique amino acid sequence of silk protein itself but also, or even more, on spinning conditions. In addition, natural silks are formed under mild physiological conditions, including an aqueous medium, ambient temperature, low hydrostatic pressure while extrusion rates and draw down ratios are both low compared with industrial polymers. These conditions are in sharp contrast to the extreme conditions including high temperature, high pressure, toxic solvents, and high draw down ratios for extruding industrial polymers.<sup>3</sup> Therefore, it is important to seek to understand the natural spinning mechanism and define the natural spinning conditions in order to develop biomimetic spinning for the production of tough silk fibers.

Most researchers agree that the natural spinning process of silk involves a conformation transition in the silk protein from random coil and/or helical conformation into  $\beta$ -sheet under shear and/or rapid elongational flow. Other factors have been found to be involved in this process. Magoshi et al. in 1990s suggested that  $\text{K}^+$  ions might be involved in the fiber formation of silkworm,<sup>19</sup> while we presented evidence that they may help to form spidroin nanofibrils in the natural spinning process for spider dragline silk.<sup>20</sup> Moreover, it has been reported that the pH value and the contents of metallic ions change progressively as silk protein flows through the secretory pathway in both spider and silkworm glands.<sup>21–23</sup> It has also been found that pH and metallic ions influence the rheology of silk protein solutions.<sup>20,24–27</sup> These findings strongly suggest that metallic ions may be important factors in natural spinning processes. In addition, metallic ions are known to influence conformation

\* To whom correspondence should be addressed: Telephone: +86-21-65642866. Fax: +86-21-65640293. E-mail, chenx@fudan.edu.cn

<sup>†</sup> The Key Laboratory of Molecular Engineering of Polymers, Department of Macromolecular Science, Fudan University.

<sup>‡</sup> Department of Material Science, National Microanalysis Center, Fudan University.

<sup>§</sup> Department of Zoology, University of Oxford.

transitions in other proteins. For instance,  $\text{Cu}^{2+}$  ions can induce the transition from helical conformation to  $\beta$ -sheet in two important and well-studied silklike proteins: Prion protein (PrP) causes fatal neurodegenerative diseases including Creutzfeldt–Jakob disease in humans and spongiform encephalopathy in animals.  $\text{Cu}^{2+}$  ions can induce conversion to the  $\beta$ -sheet-rich isoform which subsequently aggregates.<sup>28–33</sup>  $\text{Cu}^{2+}$  ions have a similar effect on amyloid  $\beta$ -peptide ( $\text{A}\beta$ ), a major constituent of senile plaques in the brains of patients with Alzheimer's disease.<sup>34–37</sup>

Although the research group lead by Magoshi reported some observations on the role of the metallic ions effect in the spinning process<sup>22,24–26,38,39</sup> in the past three years, they mainly focused on  $\text{K}^+$  and  $\text{Ca}^{2+}$ . In the present paper, we report how the contents of the six major metallic ions (Na, K, Ca, Mg, Cu, and Zn) change in the secretory pathway in *Bombyx mori*. We also describe the in vitro effects of these ions on the conformation transition of concentrated regenerated silk fibroin (CRSF) solution at a silk protein concentration similar to that in natural silk fibroin (SF) dope in vivo, about 26% (w/w). The main purpose of this research is to obtain evidence that suggests that metallic ions play a part in the conformation transition in silkworm SF in vivo. Any effect of ions on the conformation transition of CRSF solution is likely to be less pronounced than the effect of shear and/or rapid elongational flow, the major driving force for SF conformation transition in silk formation in the natural spinning process.<sup>17</sup>

## 2. Experimental Section

**2.1. Preparation of *B. mori* Silk Gland Samples.** Whole silk glands were dissected from mature fifth instar *B. mori* silkworms approximately 12 h before commencement of spinning. The epithelium was not removed from the gland to reduce the risk of loss of metallic ions from the luminal contents. The gland was briefly rinsed with deionized water to remove haemolymph, and then blotted with tissue paper. The silk gland is divided into three divisions: posterior (P) division, middle (M) division, and anterior (A) division. The wide M division serves as a reservoir for SF with a concentration as high as 26% (w/w) and is further divided into three parts, the posterior (MP), the middle (MM) and the anterior (MA).<sup>19,38</sup> In this study, we used both the whole M division as well as the separate MP, MM, MA parts for measurements of the contents of metallic elements. After blotting with filter paper, the whole M divisions and the separated parts were transferred directly to a glass weighing bottle and dried in an oven at 80 °C to constant weight.

In addition, the epithelium of some silk glands was dissected from the stiffly gelled luminal contents and discarded. To remove sericin, the luminal contents allowed to stand in deionized water (6 × 5 min changes) at 4 °C with occasional gentle agitation.

**2.2. Proton Induced X-ray Emission (PIXE) Measurements.** PIXE was used to determine K, Ca, Cu, and Zn content in silk glands. The experimental conditions were as previously described.<sup>40</sup> All measurements were repeated 3–6 times and averaged.

**2.3. Inductively Coupled Plasma Mass Spectroscopy (ICP-MS) Measurements.** Dry silk glands were ashed in a muffle furnace at 700 °C for 4 h. The ash was quantitatively dissolved in 50% (v/v)  $\text{HNO}_3$  solution. The resulting solution was diluted with a known volume of deionized water. The measurements were performed with a VG PlasmaQuad 3 ICP-MS using the following conditions: power, 1350 W; detection mode, pulse counting. All measurements were repeated 3–6 times and averaged.

**2.4. Atomic Adsorption Spectroscopy (AAS) Measurements.** The treatment of dry silk glands was the same as for ICP-MS. The measurements were performed with a Unicam Solaar 939 AAS. For Cu and Zn, a graphite furnace AAS (GFAA) method was used. For the rest of elements, a flame AAS (FAA) method was used. The air–acetylene flame was used for Na, Mg, and K, and the  $\text{N}_2\text{O}$ –acetylene flame for Ca. All measurements were repeated 3–6 times and averaged.

**2.5. Effect of Metallic Ions on the Conformation Transition of SF.** A 26% (w/w) regenerated silk fibroin (CRSF) solution was prepared according to the method described in our Chinese Patent (CN 1483866A): degummed silkworm silk fibers were first dissolved in 9.5 mol/L LiBr aqueous solution. Then, the SF LiBr solution was dialyzed against aqueous poly(ethylene glycol) (PEG) solution to obtain the final CRSF solution. The CRSF solution was placed in 25 mm wide dialysis tubes (MWCO 14 kDa; each tube containing 2 g of SF dry weight) before dialysis against 50 mL of metallic salt aqueous solution with different molar concentrations. Thus, the molar concentration of each metallic salt solution changed as a variable during the experiment corresponds to the change on mass ratio (hereafter abbreviated “ratio”) of metallic ion to SF. The dialysis was continued for 5 h to allow for the establishment of a salt–protein equilibrium. The dialysate contained one of the following metallic salts: NaCl, KCl,  $\text{MgCl}_2$ ,  $\text{CaCl}_2$ ,  $\text{CuCl}_2$ , or  $\text{ZnSO}_4$ .

To prepare natural SF dope immersed in standard metallic ion solutions, pieces of gelled dope obtained as described above were transferred with clean stainless steel watchmaker's forceps to 1.0 mol/L aqueous solutions of each metallic ion listed above for 10 min before recording Raman spectra as described below.

**2.6. Raman Spectroscopy and Semiquantitative Analysis.** Raman spectra of CRSF solutions and natural silk dope were recorded with a Dilor LabRam-1B Raman microscope. Either CRSF solution or natural silk dope was put in a flat glass well under the microscope. A He–Ne laser was used to give 6 mW of energy at 632.81 nm.

In this paper, we mainly focused on the amide I region because of its high intensity and little interference from other molecular vibrations. In amide I, the following attributions on SF are commonly employed:  $1670 \pm 5 \text{ cm}^{-1}$  is assigned to  $\beta$ -sheet,  $1655 \pm 5 \text{ cm}^{-1}$  to random coil and/or helical conformation (hereafter shortened to “random coil”), and  $1680 \pm 5 \text{ cm}^{-1}$  to an intermediate conformation between random coil and  $\beta$ -sheet.<sup>41–43</sup> As most of Raman spectra we observed were broad and with low resolution, we used the Levenberg–Marquardt algorithm to obtain an estimate of the quantity of each secondary structure in SF under different defined conditions (see above). This method has been used elsewhere<sup>44</sup> to estimate the fractions of random coil, helix,  $\beta$ -sheet, and other conformations. The wavenumbers relating to the three main components (i.e., “random coil”,  $\beta$ -sheet, and intermediate conformation) contributing to the amide I band were obtained from a second-derivative of the Raman spectra. We used the  $1615 \text{ cm}^{-1}$  band assigned to the phenyl group thought to arise mainly from the protein tyrosine residues as an invariant internal standard to check the validity of each analysis.<sup>43</sup> In most of our analyzed spectra, this internal control gave values of  $5 \pm 2\%$  of the total composition. The few spectra that gave values outside these limits were discarded.

## 3. Results and Discussion

**3.1. Contents of Metal Elements in *B. mori* Silk Gland.** More than 10 years ago, Magoshi suggested that  $\text{Ca}^{2+}$ ,  $\text{Mg}^{2+}$ , and  $\text{K}^+$  induce gelation of SF in the posterior division.<sup>19</sup> More

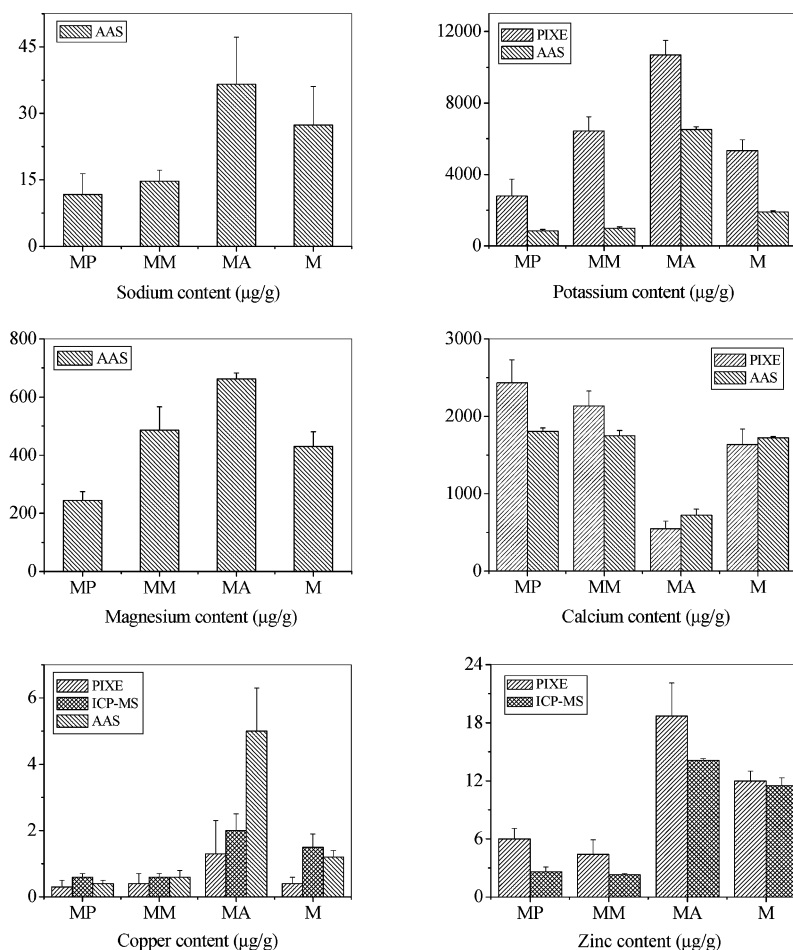


**Figure 1.** Contents of different metal elements in  $\mu\text{g/g}$  dry weight in the luminal contents in different regions (see Experimental Section) of the *B. mori* silk gland detected by PIXE, ICP-MS and AAS.

recently Magoshi's group reported the contents of K, Ca, Mg, Mn, Fe, Si, P, S, and Cl in both the silk gland and cocoon silk of *B. mori*.<sup>22</sup> In the present communication we report how Na, K, Mg, Ca, Cu, and Zn element composition changed in different parts of the middle division (Figure 1). We were unable to quantify all the elements with all the three methods at our disposal. Among the reasons for this was the fact that Na and Mg are too light for the PIXE method we employed and the amounts of K and Ca were too high for ICP-MS. Where it was possible to use two or more methods to determine the concentration of an element, we found that although the measured element composition varied somewhat from method to method, there was a reasonable correlation and all methods gave results with the same order of magnitude for a given element in a given location.

K and Ca were the most abundant elements in the gland; both elements reaching as much as several milligrams per gram in some regions. This could account for the detection of only these two metal elements by other research groups using less sensitive methods.<sup>19,25,26,38,39</sup> All the metal elements with the exception of Ca increased in content from MP to MA in accordance with the results reported by Magoshi et al.<sup>38</sup> In spider *Nephila*, we also found the K content increased along the secretory pathway, but the Na content decreased.<sup>21,45</sup> However, comparing the Na content in silkworm gland with that of the spider, the silkworm had much lower Na content, approximately  $30 \mu\text{g/g}$  compared with  $3100 \mu\text{g/g}$  in the spider, and the change in content along the secretory pathway increased in the silkworm but decreased in the spider. This may imply some differences

in spinning mechanism in these two only distantly related organisms. Finally it is of interest that in addition to the six elements discussed above that Mn and Fe were also detected in trace amounts in the *B. mori* silk gland contents.

The variation of metal element contents in different parts of silk gland and silk fiber<sup>21,22,39,45,46</sup> suggests that these ions may be involved in providing the right conditions for safe storage and formation of the solid silk in the spinning process in vivo. Accordingly, we used Raman spectroscopy to study the influence of these metallic ions on the conformation transition of CRSF solution in vitro.

### 3.2. Effects of Metallic Ions on the SF Conformation.

Raman spectroscopy provides a useful method to determine the secondary structures in SF.<sup>43,47–50</sup> Though Raman spectroscopy is limited by the low signal-to-noise ratio ( $S/N$ ) and the broadness of the bands, it is the most practical one for this study as other common methods to study the conformation transition of SF, such as CD (requires dilute solutions) and FTIR (requires  $\text{D}_2\text{O}$  as solvent) are not suitable for CRSF solution. We admit that this approach provides only approximate values because of the nature and resolution of Raman spectroscopy and the limits to the reliability of deconvolution analysis of the amide I band. However, the validity of the deconvolution method is supported by the consistency of values for the internal standard (see above) and the data for the effects of  $\text{Cu}^{2+}$  and  $\text{Na}^+$  ions, which shows that increasing the ion concentration produces progressive and consistent effects on the contents of the different secondary structures (see below). Using this method, we obtained values for the average percentage composition of each

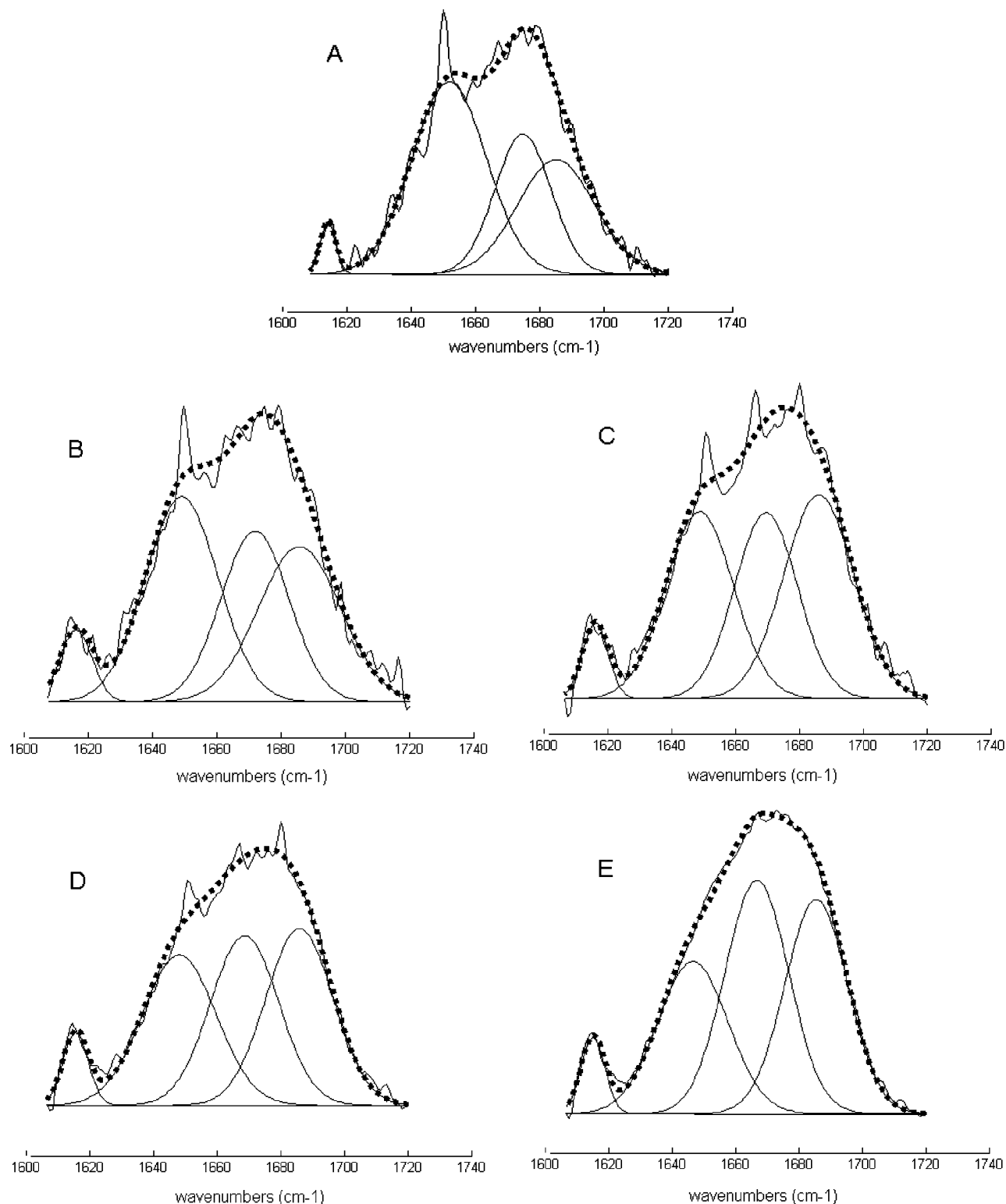


**Figure 2.** An example of the quantitative analysis of the amide I band for CRSF solution using the Levenberg–Marquardt algorithm: (A) neat CRSF solution; (B–E) treated with different  $\text{CuCl}_2$  aqueous solution.  $\text{Cu}^{2+}/\text{SF}$  ratio (w/w): (B)  $1.6 \times 10^{-5}$ ; (C)  $1.6 \times 10^{-3}$ ; (D)  $8.0 \times 10^{-3}$ ; (E) 0.8. The figure shows the original spectrum (solid line), the simulated spectra (dotted line), and their deconvoluted traces (three smooth Gaussian curves).

secondary structure in CRSF solution as follows: “random coil” 40%, the intermediate conformation 30%,  $\beta$ -sheet 25%, and the internal calibration (phenyl) 5% (Figure 2A). In comparison, the natural concentrated SF dope taken directly from the middle division gave average percentage compositions for these conformations 30%, 40%, 25%, and 5%, respectively; a somewhat lower composition of “random coil” and somewhat higher

content of the intermediate conformation were observed. This showed the “random coil” and intermediate conformations predominated in both natural dope and CRSF solution.

**3.2.1. Effects of Copper and Zinc on CRSF Solution.** Although the content of Cu was much lower than that of Mg, K, and Ca, the specific activity of the  $\text{Cu}^{2+}$  ion for inducing the conformation transition was so great that Cu is likely to



have a significant effect *in vivo* in this respect. In previous work, we used visible spectrophotometry, electronic paramagnetic resonance (EPR), nuclear magnetic resonance (NMR), and Raman spectroscopy to show that  $\text{Cu}^{2+}$  ion can induce a conformation transition from “random coil” to  $\beta$ -sheet by coordination to SF macromolecules.<sup>46,51</sup> Here, we discuss in more detail the effect of varying the  $\text{Cu}^{2+}$ /SF ratios.

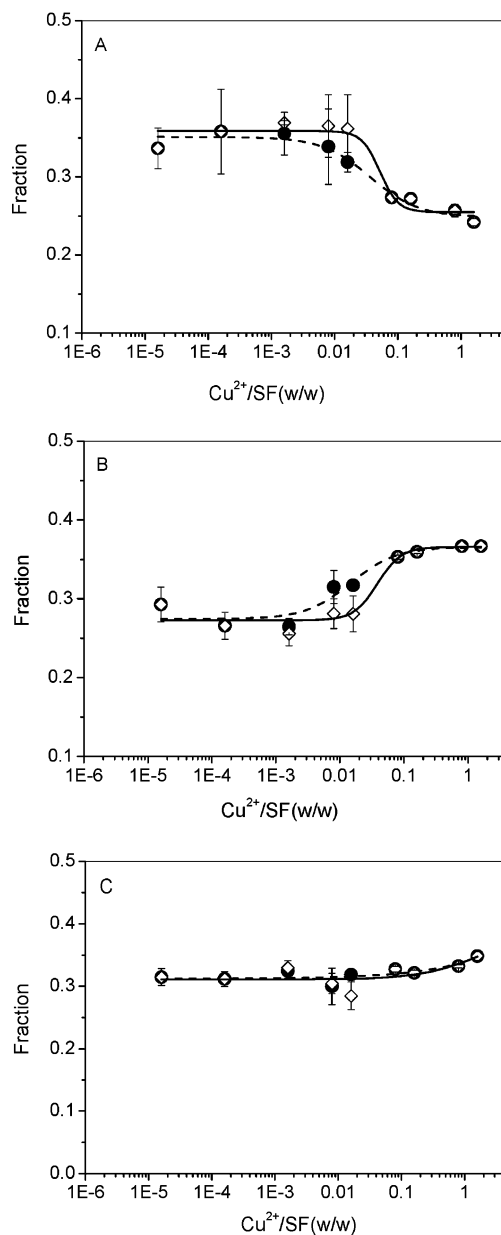
Among the six metal elements we chose to examine,  $\text{Cu}^{2+}$  ions in aqueous solution are the only ones with absorption in the visible range. With its bright blue color, we could easily show that  $\text{Cu}^{2+}$  ions attach to SF. We found it produced separation of a blue CRSF dense phase when CRSF solutions were dialyzed against  $\text{CuCl}_2$  solutions when  $\text{Cu}^{2+}$ /SF ratio was higher than  $10^{-3}$ . The underlayer of CRSF solution showed an intense blue color, suggesting the formation of an intensely colored coordination complex between the  $\text{Cu}^{2+}$  ions and the SF macromolecular chains.

Figure 2 shows the amide I band of Raman spectra for SF from the blue stained underlayer where there was one. It indicated that, with the increase in  $\text{Cu}^{2+}$ /SF ratio, the  $\beta$ -sheet fraction in the amide I band increased. When  $\text{Cu}^{2+}$ /SF ratio was low ( $\sim 10^{-5}$ ), the shape of amide I band of Raman spectra (Figure 2B) was similar to that of neat CRSF solution (Figure 2A), in which the “random coil” dominated. In contrast, when  $\text{Cu}^{2+}$ /SF ratio increased to about 1.0, the  $\beta$ -sheet fraction dominated (Figure 2E). Although the accuracy of the deconvolution method is admittedly limited (see above), the progressive nature of the changes in “random coil” and  $\beta$ -sheet fractions support the suggestion that the  $\text{Cu}^{2+}$  ions are capable of inducing a conformation transition to the  $\beta$ -sheet.<sup>46,51</sup> The separation of CRSF solution is likely to result from an increase in density resulting from both the binding of  $\text{Cu}^{2+}$  ions and the conversion of the predominantly “random coil” form to the denser  $\beta$ -sheet form together with an aggregation resulting from the formation of intermolecular  $\beta$ -sheet hydrogen bonds.

Figure 3 shows the effect of  $\text{Cu}^{2+}$ /SF ratio on the fraction of each conformation in the amide I band. Generally, in both samples from the bottom and the top of the CRSF solution, there was a sharp decrease in “random coil” coupled with an increase in  $\beta$ -sheet when  $\text{Cu}^{2+}$ /SF ratio went from approximately  $10^{-3}$  to 0.1 followed by a slower increase approaching asymptotic values at higher  $\text{Cu}^{2+}$ /SF ratio as substantially all the fibroin was converted to the  $\beta$ -sheet form.

The differences between the “random coil” and  $\beta$ -sheet fraction curves of SF from the top and the bottom of CRSF solution can be explained in terms of the effect of a progressive coordination of  $\text{Cu}^{2+}$  ions onto SF macromolecules with the increase of  $\text{Cu}^{2+}$ /SF ratio. The coordination of  $\text{Cu}^{2+}$  to SF and the formation of  $\beta$ -sheet were detectable when  $\text{Cu}^{2+}$ /SF  $> 1.6 \times 10^{-3}$  at the bottom of CRSF solution, while no changes were noted at the top of the solution. When  $\text{Cu}^{2+}$ /SF  $> 1.6 \times 10^{-2}$ , most of the SF was coordinated with  $\text{Cu}^{2+}$  ions, so that the increase of  $\beta$ -sheet can also be detected on the top of the CRSF solution. In comparison, the proportion of the intermediate conformation changed little until the  $\text{Cu}^{2+}$ /SF  $> 1.6 \times 10^{-2}$ , thereafter increasing slightly with the increase of  $\text{Cu}^{2+}$ /SF ratio. This suggests that the intermediate state is not formed in a constant proportion to the  $\beta$ -sheet conformation.

In our previous studies,<sup>46</sup> we presented evidence that  $\text{Cu}^{2+}$  ion started to coordinate to SF macromolecular chains when the  $\text{Cu}^{2+}$ /SF ratio was between  $4 \times 10^{-4}$  and  $4 \times 10^{-3}$ , close to the value (between  $1.6 \times 10^{-3}$  and  $1.6 \times 10^{-2}$ ) required to initiate the induction of the conformation transition to  $\beta$ -sheet as reported above. The slight difference between these two



**Figure 3.** Fraction of different conformations of the CRSF solution with different  $\text{Cu}^{2+}$ /SF ratio (from the bottom of the CRSF solution, ● and dash line; from the top of the CRSF solution, ◇ and solid line: (A) “random coil” at  $1650\text{ cm}^{-1}$ ; (B)  $\beta$ -sheet at  $1667\text{ cm}^{-1}$ ; (C) intermediate conformation at  $1680\text{ cm}^{-1}$ ).

values may result from differences in the two experimental methods, the former only considering coordination of  $\text{Cu}^{2+}$  ions onto SF macromolecular chains and not conformational change induced by this.

$\text{Cu}^{2+}$  ions can induce  $\beta$ -sheet formation in SF as discussed in our previous paper.<sup>46,51</sup> Histidine is known to form coordination complexes with transition metals and we suggested that the three repeats of the histidine-containing motif AHGGYSGY in silk fibroin may be the coordination site of  $\text{Cu}^{2+}$  ions as it is somewhat similar to the highly conserved PHGGGWGQ in PrP thought to be particularly important for binding  $\text{Cu}^{2+}$  ions. From the Cu content of silk protein in the MA part of the *B. mori* silk gland ( $2.0\text{ }\mu\text{g/g}$ ) and silk fiber ( $4.5\text{ }\mu\text{g/g}$ ),<sup>46</sup> we calculate that the ratio of  $\text{Cu}^{2+}$  ion number to histidine residue ( $\text{Cu}^{2+}$ /His) in SF<sup>51</sup> *in vivo* was about 1/230 in MA part of silk gland and 1/100 in silk fiber. Therefore, the great excess of SF may ensure that every  $\text{Cu}^{2+}$  ions is bound to a AHGGYSGY motif

in vivo. The very low ratio in vivo suggests that only a tiny fraction of the SF molecules need to bind  $\text{Cu}^{2+}$  ions to play a facilitating role in the strain-induced formation of  $\beta$ -sheet. We showed in a previous study<sup>46</sup> that the minimum  $\text{Cu}^{2+}$ /His ratio required for coordination between  $\text{Cu}^{2+}$  ions and SF was 0.9 while in the present study a somewhat higher ratio (3.4) but of the same order of magnitude was required to induce the conformation transition. The difference may result from the different parameters measured in the two studies, the former measuring the coordination between  $\text{Cu}^{2+}$  ions and SF and the present study, the conformation transition of SF.

Both Zn and Cu are transition metal elements and both are capable of binding to the same amino acid residues in proteins. Accordingly we sought to discover whether  $\text{Zn}^{2+}$  ions could also induce a conformation transition in CRSF solution. A much higher ratio of  $\text{Zn}^{2+}$ /SF was found to be required to initiate the conformation transition compared with  $\text{Cu}^{2+}$  ions (figure not shown). When the  $\text{Zn}^{2+}$ /SF ratio was increased from  $10^{-5}$  to 1, the “random coil” proportion decreased from approximately 40% to 32%, the  $\beta$ -sheet proportion increased from approximately 25% to 31% and the intermediate proportion showed little change (from 30% to 32%).

$\text{Zn}^{2+}$  ions compared with  $\text{Cu}^{2+}$  ions showed a weaker effect on the conformation transition in PrP and A $\beta$  as reported by Stockel et al.<sup>28</sup> These authors showed that the binding sites of PrP were highly specific for  $\text{Cu}^{2+}$  ions and do not bind other metal ions such as  $\text{Zn}^{2+}$ ,  $\text{Ca}^{2+}$ , and  $\text{Mg}^{2+}$ . Aggregation studies on A $\beta$  also indicated that the  $\text{Cu}^{2+}$  ion has a relatively specific ability to induce the aggregation of soluble A $\beta$  at pH 6.8.<sup>34</sup> This could explain the difference in sensitivity of SF to  $\text{Zn}^{2+}$  and  $\text{Cu}^{2+}$  ion and, as the silkworm diet is likely to contain much more Zn than Cu, of the advantage of having a Zn content 10 times larger than Cu in the *B. mori* silk gland (see above).

**3.2.2. Effects of Calcium and Magnesium on CRSF Solution.** We have shown above that the Ca content falls in the secretory pathway in *B. mori* while the other five elements increased (Figure 1). Accordingly we investigated the effect of  $\text{Ca}^{2+}$  ions on conformations in CRSF solution in vitro. We used  $\text{Ca}^{2+}$ /SF ratio from  $10^{-3}$  to 3 as the Ca content was quite high in the silk gland. Figure 4 illustrates the effect of  $\text{Ca}^{2+}$  ions on each conformation fraction in CRSF solution. Although the number of data points and the size of the apparent effect are both small, the data gives a preliminary indication that  $\text{Ca}^{2+}$  ions may have an effect on the secondary structure of SF.

The fraction of conformations in SF at the lowest  $\text{Ca}^{2+}$ /SF ratio ( $10^{-3}$ ) were not significantly different from those in the control (neat) CRSF solution but there was a suggestion of a sudden decrease in “random coil” with increasing  $\text{Ca}^{2+}$ /SF ratio and a sudden increase in intermediate fraction which plateaued at a  $\text{Ca}^{2+}$ /SF ratio between  $10^{-3}$  and  $10^{-2}$ . This plateau for the intermediate conformation was appreciably higher (35%) compared to the equivalent value (30%) for the control CRSF solution. This increase in the intermediate conformation may be derived from the decrease in “random coil” conformation (from 40% to 35%). Taken together these observations indicates that the intermediate conformation maybe favored at a  $\text{Ca}^{2+}$ /SF ratio corresponding to the value of 2.0 mg/g we found in the gland (see above).

Magoshi et al. recently proposed that  $\text{Ca}^{2+}$  ions favor the gelation and stable storage of the liquid silk gel in *B. mori* silk gland lumen,<sup>25,52</sup> while Chronakis's study of the effect of  $\text{Ca}^{2+}$  ions on soy protein dispersions indicates that  $\text{Ca}^{2+}$  ions can stabilize the structure of partially denatured soy protein gels.<sup>53</sup> In addition, a number of reports indicate that  $\text{Ca}^{2+}$  ion-binding

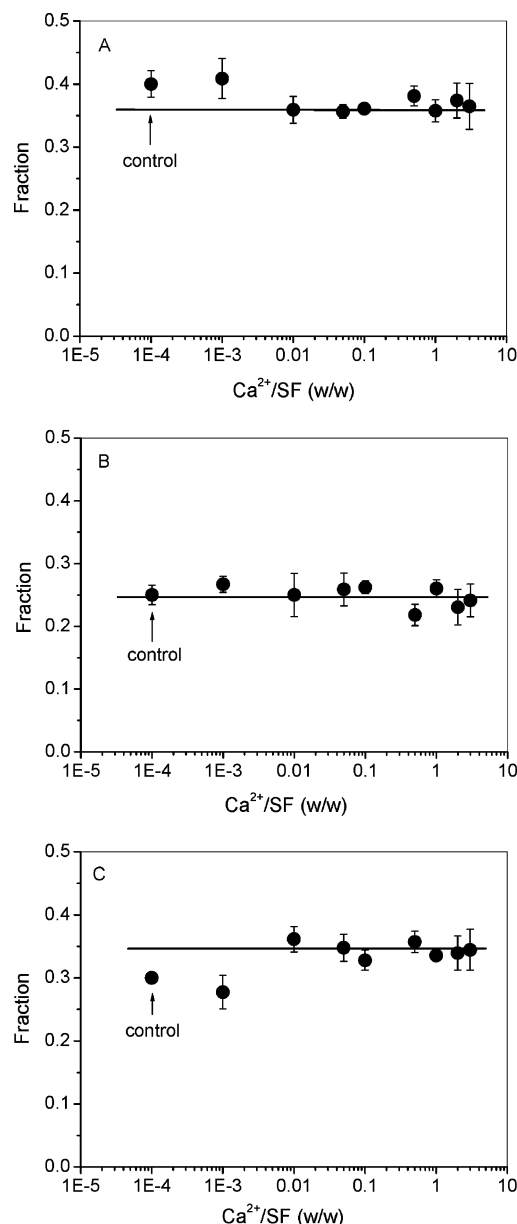


**Figure 4.** Fraction of different conformations of CRSF solution with different  $\text{Ca}^{2+}$ /SF ratio: (A) “random coil” at  $1650\text{ cm}^{-1}$ ; (B)  $\beta$ -sheet at  $1667\text{ cm}^{-1}$ ; (C) intermediate conformation at  $1680\text{ cm}^{-1}$ .

has no effect on the secondary structure of proteins<sup>54–56</sup> or do not favor the  $\beta$ -sheet conformation.<sup>57,58</sup> Therefore, we suggest the  $\text{Ca}^{2+}$  ions at concentrations found in the MP and MM of the gland may stabilize SF in a gel state by forming the intermediate conformation between “random coil” and  $\beta$ -sheet, possibly a distorted  $\beta$ -sheet structure held together by  $\text{Ca}^{2+}$  ions.

Our data suggest that  $\text{Ca}^{2+}$  ions are not favorable to  $\beta$ -sheet formation. The relatively high Ca content in the MP and MM may facilitate the safe storage of the protein in a stable gel form which does not readily convert to the  $\beta$ -state. Further, a reduction in Ca content as the material flows on through the secretory pathway (MA and A division) may permit the formation of the  $\beta$ -state, encouraging the formation of the insoluble thread. A similar suggestion has been made on the basis of a study of the reversible gelation of natural *B. mori* silk dope taken from the lumen of the middle division of the gland.<sup>27</sup>

The content of Mg was much less than Ca in the MP and MM of the silk gland, but almost equal to that of Ca in the

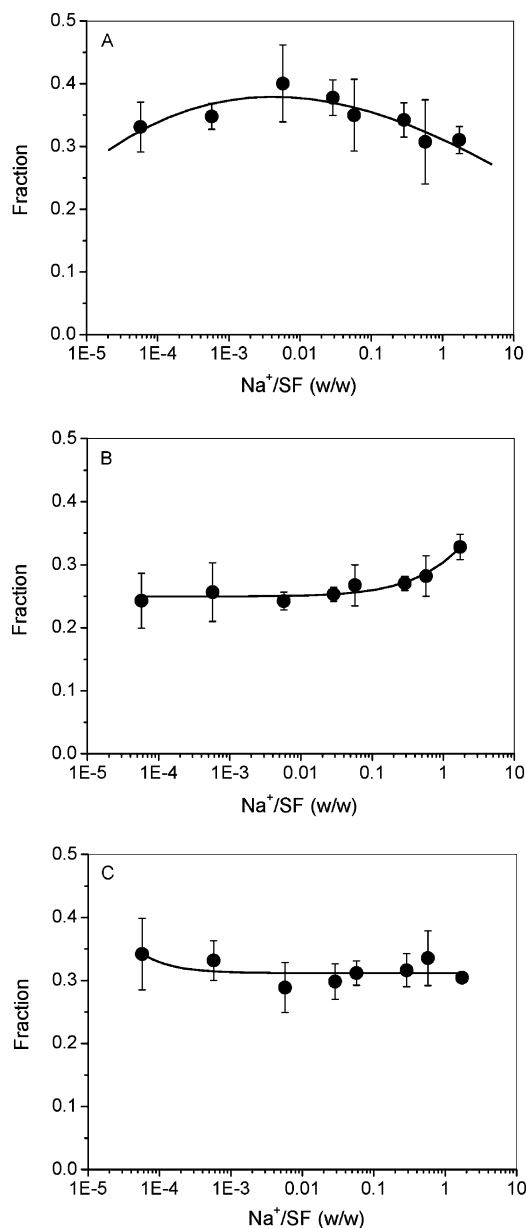


**Figure 5.** Fraction of different conformations of CRSF solution with different  $\text{Na}^+/\text{SF}$  ratio. (A) “random coil” at  $1650\text{ cm}^{-1}$ ; (B)  $\beta$ -sheet at  $1667\text{ cm}^{-1}$ ; (C) intermediate conformation at  $1680\text{ cm}^{-1}$ .

MA.  $\text{Mg}^{2+}$  ions, like  $\text{Ca}^{2+}$  ions had only a small effect on the conformations of CRSF solutions. Increasing the  $\text{Mg}^{2+}/\text{SF}$  ratio may have a slight effect on the conformations present: a slight decrease in the “random coil” fraction coupled with a slight increase in  $\beta$ -sheet fraction (figure not shown). Uversky et al. also found  $\text{Mg}^{2+}$  ions resulted in a small increase in ordered secondary structure in human  $\alpha$ -synuclein.<sup>56</sup> Thus, their findings may be similar to those we obtained for SF.

### 3.2.3. Effects of Sodium and Potassium on CRSF Solution.

The effect of  $\text{Na}^+$  ions on the conformations in CRSF solution is illustrated in Figure 5. The “random coil” fraction reached a maximum value when  $\text{Na}^+/\text{SF}$  ratio was about  $6.0 \times 10^{-3}$ . Lowering the  $\text{Na}^+/\text{SF}$  ratio beneath this value resulted in a reduction in the “random coil” fraction arising mainly from an increase in the intermediate component. Increasing  $\text{Na}^+/\text{SF}$  ratio above  $6.0 \times 10^{-3}$  resulted in the conversion of “random coil” to  $\beta$ -sheet. The Na content of the silk gland is quite low (see Figure 1 above), giving a  $\text{Na}^+/\text{SF}$  ratio of considerably less than  $6.0 \times 10^{-3}$ . If the natural SF behaves like the regenerated SF,

the observed increase of Na content from the MP to the MA part of the silk gland would have the effect of increasing “random coil” and decreasing the intermediate conformation. Thus, as the  $\text{Na}^+$  ions increase and  $\text{Ca}^{2+}$  ions decrease as the silk protein flows through the secretory pathway, the effect of these two ionic changes might be additive as both changes would appear to result in an increase of “random coil” and decrease of intermediate conformation.

Although K had the highest content of the six metal elements determined, it had little effect on the conformation change of CRSF solutions at any  $\text{K}^+/\text{SF}$  ratio (results not shown). However, though  $\text{Na}^+$  and  $\text{K}^+$  ions lack an effect on the CRSF solutions, they may have an effect on natural SF solutions. In this connection it is interesting to note that alkaline metal ions have been shown to have two effects on natural spidroin (spider fibroin) solutions: (i) In a previous study both  $\text{K}^+$  and  $\text{Na}^+$  ions appear to enhance the  $\beta$ -sheet transition,<sup>59</sup> and (ii)  $\text{K}^+$  ions but not  $\text{Na}^+$  ions appear to induce nanofibril in formation.<sup>20</sup> Any difference in the action of ions on natural as compared with regenerated silk may arise from differences in tertiary and/or secondary structure in these two very different types of solution. To investigate this possibility we investigated the effect of ions on natural SF dope.

### 3.2.4. Effect of Metallic Ions on Natural *B. mori* SF Dope.

Metallic ions were added to natural *B. mori* SF dope obtained directly from the middle division of the silk gland (see Experimental Section). Addition of  $1.0\text{ mol/L}$   $\text{Cu}^{2+}$  or  $\text{Zn}^{2+}$  ion solutions produced a fibrous precipitate on the surface of the natural SF dope. Surprisingly we found that the addition of  $1.0\text{ mol/L}$   $\text{K}^+$  ions solution was able to accelerate the dissolution of the natural SF dope.  $\text{Na}^+$ ,  $\text{Ca}^{2+}$ , and  $\text{Mg}^{2+}$  ions had no apparent effect on the protein solubility. The selectivity of  $\text{K}^+$  ions in this respect may result from their greater ability compared to  $\text{Na}^+$  ions to enhance the breakdown of the gel silk protein network as a result of their higher position on the Hoffmeister series for cations. Increased Coulombic forces produced by the twin positive charges of  $\text{Ca}^{2+}$  and  $\text{Mg}^{2+}$  ions may prevent the breakdown of the gel network by complexing between the negatively charged SF macromolecules. A possible candidate for the site of the gel-forming and stabilizing interactions produced by  $\text{Ca}^{2+}$  ions are the Glu-Ser-Asp triplets present in the most of the hydrophilic spacers in the SF heavy chain molecule, or the many aspartic acids located in the N-terminus.

Figure 6 shows the Raman spectra of natural SF dope with and without metallic ions. With the addition of  $\text{K}^+$  ions, the Raman spectra (curve B, similar to  $\text{Na}^+$  and  $\text{Mg}^{2+}$  ions) was closely similar to that of neat dope (curve A).  $\text{Ca}^{2+}$  ion addition produced a marked reduction of the  $\beta$ -sheet peak (curve C). As in CRSF solution,  $\text{Cu}^{2+}$  ion addition produced a mark increase in  $\beta$ -sheet in natural SF dope. The center of amide I band shifted to  $1667\text{ cm}^{-1}$  (curve D) characteristic of  $\beta$ -sheet, and the bands at both  $1652$  and  $1681\text{ cm}^{-1}$  were significantly weakened. Similar changes were produced by the addition of  $\text{Zn}^{2+}$  ions to natural SF dope.

It is of interest that  $\text{K}^+$  ions help the dissolution of natural SF dope but induce the precipitation of nanofibrils in natural *Nephila* spidroin solutions probably by converting the  $\alpha$ -helix/random coil form to the  $\beta$ -sheet.<sup>20,45</sup> However, in *B. mori* SF,  $\text{K}^+$  ions may help the breakdown of the gel network, having the opposite effect to  $\text{Ca}^{2+}$  ions. Therefore, the increase of K content as well as the decrease of Ca content in anterior part of silk gland may promote the break down of the stable gel formed in the middle part of silk gland, allowing SF macromolecular



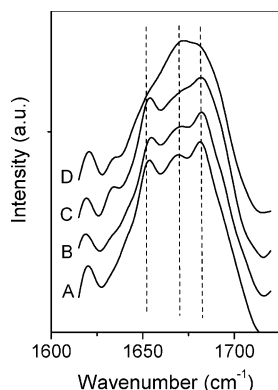


**Figure 6.** Raman spectra about various metallic ions effects on the natural SF dope. (A) control; (B) sample with 1.0 mol/L  $K^+$  ions; (C) sample with 1.0 mol/L  $Ca^{2+}$  ions; (D) sample with 1.0 mol/L  $Cu^{2+}$  ions.

chains to move more freely, enabling the dope to flow through the anterior division while permitting subsequent  $\beta$ -sheet (silk fiber) formation.

#### 4. Conclusions

We report above the presence of six metal elements (Na, K, Mg, Ca, Cu, and Zn) in the luminal contents of the *B. mori* silkworm silk gland. The contents of each of these elements appeared to increase from posterior part to anterior part of silk gland with the exception of Ca which dropped dramatically in the anterior part. Accordingly, we investigated the effects of the ions at different concentrations on the secondary structures in CRSF solution by deconvoluting the amide I band in Raman spectra. We also carried out a similar preliminary qualitative examination of the effects of these ions on natural SF dope prepared directly from the silk gland. According to the results we obtained here and those already published, we may come to the following conclusions. Different metallic ions have their own different effects on the conformation transition of SF. These effects may correlate with their distribution in different parts of the silk gland and with their role in the spinning process in vivo. In general,  $Mg^{2+}$ ,  $Cu^{2+}$ , and  $Zn^{2+}$  ions appeared to be favorable to  $\beta$ -sheet formation and their contents increased from MP to MA part in silk gland.  $K^+$  ions were apparently able to break down the stable gel network of natural SF while  $Ca^{2+}$  ions helped to maintain it. This suggests that the increase in Na and K content from MP to MA part of silk gland and the decrease in Ca content both serve to weaken the stable gel and prepare natural SF macromolecules for  $\beta$ -sheet formation in the distal part of the silkworm's anterior division.

These findings may have important implications for our understanding of natural spinning process and may assist in the ultimate development of artificial methods for spinning strong fibers from silklike proteins.

**Acknowledgment.** This work is supported by the National Natural Science Foundation of China (Nos. 50373006 and 20434010) and the Excellent Young Teachers Program of MOE of China. We thank Dr. Ping Zhou and Dr. Jinrong Yao for helpful advice and discussion. We also thank Prof. Hao Shen of the Institute of Modern Physics and Prof. Wenhua Yao of the Research Center of Analysis and Measurement of Fudan University for the help on PIXE and Raman measurements as well as Prof. Junting Huang of Sericultural Research Institute, Chinese Academy of Agricultural Science for the kind supply of silkworms.

#### References and Notes

- (1) Gosline, J. M.; DeMont, M. E.; Denny, M. W. *Endeavour* **1986**, 10, 31.
- (2) Tirrell, D. A. *Science* **1996**, 271, 39.
- (3) Shao, Z. Z.; Vollrath, F. *Nature (London)* **2002**, 418, 741.
- (4) Hinman, M. B.; Jones, J. A.; Lewis, R. V. *Trends Biotechnol.* **2000**, 18, 374.
- (5) Vollrath, F.; Knight, D. P. *Nature* **2001**, 410, 541.
- (6) Craig, C. L.; Riekel, C. *Comp. Biochem. Physiol. B: Biochem. Mol. Biol.* **2002**, 133, 493.
- (7) Zhou, C. Z.; Confalonieri, F.; Medina, N.; Zivanovic, Y.; Esnault, C.; Yang, T.; Jacquet, M.; Janin, J.; Duguet, M.; Perasso, R.; Li, Z. G. *Nucleic Acids Res.* **2000**, 28, 2413.
- (8) Zhou, C. Z.; Confalonieri, F.; Jacquet, M.; Perasso, R.; Li, Z. G.; Janin, J. *Proteins* **2001**, 44, 119.
- (9) Lazaris, A.; Arcidiacono, S.; Huang, Y.; Zhou, J. F.; Duguay, F.; Chretien, N.; Welsh, E. A.; Soares, J. W.; Karatzas, C. N. *Science* **2002**, 295, 472.
- (10) Cappello, J.; McGrath, K. P. In *Silk Polymers*; Kaplan, D., Adams, W. W., Farmer, B., Viney, C., Eds.; American Chemical Society: Washington, 1994; Vol. 544, p 311.
- (11) Cappello, J.; Crissman, J.; Dorman, M.; Mikolajczak, M.; Textor, G.; Marquet, M.; Ferrari, F. *Biotechnol. Prog.* **1990**, 6, 198.
- (12) Cappello, J. *MRS Bull.* **1992**, 17, 48.
- (13) Liivak, O.; Blye, A.; Shah, N.; Jelinski, L. W. *Macromolecules* **1998**, 31, 2947.
- (14) Seidel, A.; Liivak, O.; Jelinski, L. W. *Macromolecules* **1998**, 31, 6733.
- (15) Seidel, A.; Liivak, O.; Calve, S.; Adaska, J.; Ji, G. D.; Yang, Z. T.; Grubb, D.; Zax, D. B.; Jelinski, L. W. *Macromolecules* **2000**, 33, 775.
- (16) Shao, Z. Z.; Vollrath, F.; Yang, Y.; Thgersen, H. C. *Macromolecules* **2003**, 36, 1157.
- (17) Knight, D. P.; Vollrath, F. *Proc. R. Soc. London Ser. B—Biol. Sci.* **1999**, 266, 519.
- (18) Vollrath, F.; Madsen, B.; Shao, Z. Z. *Proc. R. Soc. London, Ser. B: Biol. Sci.* **2001**, 268, 2339.
- (19) Magoshi, J.; Magoshi, Y.; Nakamura, S. In *Silk Polymers*; Kaplan, D., Adams, W. W., Farmer, B., Viney, C., Eds.; American Chemical Society: Washington, DC, 1994; Vol. 544, p 292.
- (20) Chen, X.; Knight, D. P.; Vollrath, F. *Biomacromolecules* **2002**, 3, 644.
- (21) Knight, D. P.; Vollrath, F. *Naturwissenschaften* **2001**, 88, 179.
- (22) Tanaka, T.; Magoshi, J.; Magoshi, Y.; Inoue, S. I.; Kobayashi, M.; Tsuda, H.; Nakamura, S. *Abstr. Pap. Am. Chem. Soc.* **2001**, 221, 123.
- (23) Dicko, C.; Vollrath, F.; Kenney, J. M. *Biomacromolecules* **2004**, 5, 704.
- (24) Ochi, A.; Nemoto, N.; Magoshi, J.; Ohya, E.; Hossain, K. S. J. *Soc. Rheol. Jpn.* **2002**, 30, 289.
- (25) Ochi, A.; Hossain, K. S.; Magoshi, J.; Nemoto, N. *Biomacromolecules* **2002**, 3, 1187.
- (26) Kobayashi, M.; Tanaka, T.; Inoue, S.; Tsuda, H.; Magoshi, J.; Magoshi, Y.; Becker, M. A. *Abstr. Pap. Am. Chem. Soc.* **2001**, 222, 113.
- (27) Terry, A. E.; Knight, D. P.; Porter, D.; Vollrath, F. *Biomacromolecules* **2004**, 5, 768.
- (28) Stockel, J.; Safar, J.; Wallace, A. C.; Cohen, F. E.; Prusiner, S. B. *Biochemistry* **1998**, 37, 7185.
- (29) Aronoff-Spencer, E.; Burns, C. S.; Avdievich, N. I.; Gerfen, G. J.; Peisach, J.; Antholine, W. E.; Ball, H. L.; Cohen, F. E.; Prusiner, S. B.; Millhauser, G. L. *Biochemistry* **2000**, 39, 13760.
- (30) Burns, C. S.; Aronoff-Spencer, E.; Dunham, C. M.; Lario, P.; Avdievich, N. I.; Antholine, W. E.; Olmstead, M. M.; Vrieling, A.; Gerfen, G. J.; Peisach, J.; Scott, W. G.; Millhauser, G. L. *Biochemistry* **2002**, 41, 3991.
- (31) Burns, C. S.; Aronoff-Spencer, E.; Legname, G.; Prusiner, S. B.; Antholine, W. E.; Gerfen, G. J.; Peisach, J.; Millhauser, G. L. *Biochemistry* **2003**, 42, 6794.
- (32) Millhauser, G. L. *Acc. Chem. Res.* **2004**, 37, 79.
- (33) Jobling, M. F.; Huang, X. D.; Stewart, L. R.; Barnham, K. J.; Curtain, C.; Volitakis, I.; Perugini, M.; White, A. R.; Cherny, R. A.; Masters, C. L.; Barrow, C. J.; Collins, S. J.; Bush, A. I.; Cappai, R. *Biochemistry* **2001**, 40, 8073.
- (34) Atwood, C. S.; Moir, R. D.; Huang, X. D.; Scarpa, R. C.; Bacarra, N. M. E.; Romano, D. M.; Hartshorn, M. K.; Tanzi, R. E.; Bush, A. I. *J. Biol. Chem.* **1998**, 273, 12817.
- (35) Bush, A. I. *Alzheimer Dis. Assoc. Dis.* **2003**, 17, 147.
- (36) Bush, A. I. *Trends Neurosci.* **2003**, 26, 207.
- (37) Miura, T.; Suzuki, K.; Kohata, N.; Takeuchi, H. *Biochemistry* **2000**, 39, 7024.
- (38) Tsuda, H.; Kobayashi, M.; Tanaka, T.; Inoue, S.; Magoshi, Y.; Magoshi, J. *Abstr. Pap. Am. Chem. Soc.* **2002**, 223, 67.
- (39) Tanaka, T.; Kobayashi, M.; Tsuda, H.; Inoue, S.; Magoshi, Y.; Nakamura, S.; Magoshi, J. *Abstr. Pap. Am. Chem. Soc.* **2002**, 223, 68.



- (40) Liu, Y.; Yu, T.; Yao, H.; Yang, F. *J. Appl. Polym. Sci.* **1997**, *66*, 405.
- (41) Tuma, R.; Parker, M. H.; Weigele, P.; Sampson, L.; Sun, Y. H.; Krishna, N. R.; Casjens, S.; Thomas, G. J.; Prevelige, P. E. *J. Mol. Biol.* **1998**, *281*, 81.
- (42) Asakura, T.; Yao, J. M.; Yamane, T.; Umemura, K.; Ultrich, A. S. *J. Am. Chem. Soc.* **2002**, *124*, 8794.
- (43) Monti, P.; Taddei, P.; Freddi, G.; Asakura, T.; Tsukada, M. *J. Raman Spectrosc.* **2001**, *32*, 103.
- (44) Trabbic, K. A.; Yager, P. *Macromolecules* **1998**, *31*, 462.
- (45) Chen, X.; Huang, Y. F.; Shao, Z. Z.; Huang, Y.; Zhou, P.; Knight, D. P.; Vollrath, F. *Chem. J. Chinese Univ.* **2004**, *25*, 1160.
- (46) Zhou, L.; Chen, X.; Shao, Z. Z.; Zhou, P.; Knight, D. P.; Vollrath, F. *FEBS Lett.* **2003**, *554*, 337.
- (47) Monti, P.; Freddi, G.; Bertoluzza, A.; Kasai, N.; Tsukada, M. *J. Raman Spectrosc.* **1998**, *29*, 297.
- (48) Shao, Z.; Vollrath, F.; Sirichaisit, J.; Young, R. J. *Polymer* **1999**, *40*, 2493.
- (49) Sirichaisit, J.; Brookes, V. L.; Young, R. J.; Vollrath, F. *Biomacromolecules* **2003**, *4*, 387.
- (50) Shao, Z. Z.; Young, R. J.; Vollrath, F. *Int. J. Biol. Macromol.* **1999**, *24*, 295.
- (51) Zong, X. H.; Zhou, P.; Shao, Z. Z.; Chen, S. M.; Chen, X.; Hu, B. W.; Deng, F.; Yao, W. H. *Biochemistry* **2004**, *43*, 11932.
- (52) Tsuda, H.; Tanaka, T.; Inoue, S.; Magoshi, Y.; Magoshi, J. *Abstr. Pap. Am. Chem. Soc.* **2003**, 225, 556.
- (53) Chronakis, I. S. *Food Res. Int.* **1996**, *29*, 123.
- (54) Saba, R. I.; Goormaghtigh, E.; Ruyschaert, J. M.; Herchuelz, A. *Biochemistry* **2001**, *40*, 3324.
- (55) Park, H. Y.; So, S. H.; Lee, W. B.; You, S. H.; Yoo, S. H. *Biochemistry* **2002**, *41*, 1259.
- (56) Uversky, V. N.; Li, J.; Fink, A. L. *J. Biol. Chem.* **2001**, *276*, 44284.
- (57) Ascoli, G. A.; Luu, K. X.; Olds, J. L.; Nelson, T. J.; Gusev, P. A.; Bertucci, C.; Bramanti, E.; Raffaelli, A.; Salvadori, P.; Alkon, D. L. *J. Biol. Chem.* **1997**, *272*, 24771.
- (58) Heredia, P.; De Las Rivas, J. *Biochemistry* **2003**, *42*, 11831.
- (59) Dicko, C.; Kenney, J. M.; Knight, D.; Vollrath, F. *Biochemistry* **2004**, *43*, 14080.